Revista Mexicana de Astronomía y Astrofísica, 62, 205-209, (2026)

OPEN ACCESS https://doi.org/10.22201/ia.30618649e.2026.62.02.7474

Benchmarking Astrochemistry Paradigms: Relative Absence of $C_6H_5CN^+$ in the Diffuse ISM

D. Majaess [1], C. Morera-Boado [2], T. A. Harriott [3], Q. Rahi[3], H. Seuret[4], L. Massa [5] and C. F. Matta [1]

[1]*Department of Chemistry and Physics, Mount Saint Vincent University, Halifax, Nova Scotia, B3M2J6 Canada.*
[2]*IXM-Secihti-Centro de Investigaciones Químicas, IICBA, Universidad Autónoma del Estado de Morelos, Cuernavaca, 62209, Morelos, México.*
[3]*Department of Mathematics and Statistics, Mount Saint Vincent University, Halifax, Nova Scotia, B3M2J6 Canada.*
[4]*Prepa TEC Campus Cuernavaca, Instituto Tecnológico y de Estudios Superiores de Monterrey, 62209, Cuernavaca, Morelos, México.*
[5]*Hunter College & the PhD Program of the Graduate Center, City University of New York, New York, USA.*

Keywords: *astrochemistry*

Abstract

The detectability of $C_6H_5CN^+$ (benzonitrile cation) in the diffuse ISM is re-evaluated. A holistic evidentiary framework suggests $C_6H_5CN^+$ is relatively absent in the diffuse ISM owing to the following reasons: marginal intramolecular vibrational energy redistribution (IVR) favoring fragmentation, recurrent fluorescence being an improbable mechanism in this case to prevent dissociation, unceasing photon strikes, mismatches between observed DIBs and experimental results, and the hitherto absence of DIBs matching any similarly sized cations. The putative gap in bottom-up synthesis is reaffirmed (diffuse ISM), and although DIB sources are largely unknown, within a broader approach, the lines can help benchmark astrochemistry paradigms. The results relied on new advantageous Daly et al. experimental spectra, an expanded observational DIB analysis (APO catalog), and complementary ωB97X-D/cc-pVTZ computations.

Resumen

En este trabajo se reevalúa la detectabilidad de $C_6H_5CN^+$ (catión benzonitrilo) en el medio interestelar difuso (ISM). Un enfoque integral basado en múltiples líneas de evidencia sugiere que $C_6H_5CN^+$ está relativamente ausente en el ISM difuso, debido a la concurrencia de los siguientes factores: una redistribución intramolecular de energía vibracional (IVR) marginal que favorece la fragmentación; la fluorescencia recurrente, que en este caso resulta un mecanismo improbable para prevenir la disociación; impactos incesantes de fotones; discrepancias entre las bandas interestelares difusas (DIBs) observadas y los resultados experimentales; y la ausencia, hasta ahora, de DIBs que coincidan con cationes de tamaño similar. Asimismo, se reafirma la existencia de una posible brecha en la síntesis ascendente en el ISM difuso y, aunque las fuentes de las DIBs son en gran medida desconocidas, en un contexto más amplio estas líneas pueden contribuir a establecer puntos de referencia para los paradigmas de la astroquímica. Los resultados se sustentan en nuevos espectros experimentales de alta calidad reportados por Daly et al., un análisis observacional ampliado de las DIBs (catálogo APO) y cálculos complementarios a nivel ωB97X-D/cc-pVTZ.

Corresponding author: Daniel Majaess *E-mail address:* Daniel.Majaess@msvu.ca
Received: November 19, 2025 **Accepted:** May 5, 2026

1. Introduction

Diffuse interstellar bands (DIBs) are a long-standing spectroscopic mystery (Heger 1922) and are tied to unknown molecules superposing absorption lines along the sightline. Less than 1% of > 550 DIBs are associated with a source, and in that case, a sole carrier is contested (C_{60}^+, see §3, and e.g., Campbell et al. 2015; Galazutdinov et al. 2021; Majaess et al. 2025a,b). Concurrently, experimental spectra, quantum chemistry predictions, and DIB catalogs can help benchmark proposed carriers. Toward that purpose, Daly et al. (2024) provided optimal laboratory spectra for the benzonitrile cation ($C_6H_5CN^+$, also referred to as BZN^+). The neutral variant was detected in cold dense molecular clouds (McGuire et al. 2018; Cernicharo et al. 2023), which inevitably motivated a comparison between the cation and DIBs. Cations are probable in the diffuse ISM owing to a low-density and unshielded environment, where higher energy photons are abundant and comparatively unobscured, thus leading to ionization (e.g., Crawford et al. 1985). Moreover, cations can produce lines in the optical where most DIBs reside, whereas certain neutral counterparts typically absorb shorter wavelengths (e.g., Weisman et al. 2003; Harriott et al. 2025; Seuret et al. 2025).

Smaller aromatics are particularly susceptible to dissociating higher energy photons present in the diffuse ISM (e.g., 6 – 13.6 eV, the interstellar radiation field, ISRF). Consequently, bottom-up synthesis of benzene ring(s) from smaller fragments may be unlikely therein (e.g. Allain et al. 1996), owing to the comparative transparency of the environment, and since ion-neutral induced dipole interactions govern simpler assembly (e.g., CH^+, CH, CN,

etc.). Benzonitrile features a low intramolecular vibrational energy redistribution (IVR) (e.g., Fig. 2 in Allain et al. 1996, and Fig. 3 in Montillaud et al. 2013, see also Rice-Ramsperger-Kassel-Marcus theory, RRKM, Marcus 1952; Di Giacomo 2015), and the balance between destruction and creation is biased toward the former. The limited vibrational density of states inherent to small molecules yields slower IVR, thus allowing the energy to funnel more quickly through dissociation. Specifically, Allain et al. (1996) concluded that aromatics containing less than 50 carbon atoms will be comparatively absent in the diffuse ISM, and Montillaud et al. (2013) support that assertion noting such molecules shall be fully dehydrogenated (e.g., benzonitrile, which has merely 7 carbon atoms). However, and importantly, it was posited in the literature that $C_6H_5CN^+$ could survive destruction via recurrent fluorescence, whereas a separate view is expressed here (§2.1). Nevertheless, IVR rapidly occurs for larger PAHs or fullerenes, as energy is redistributed among numerous modes before fragmentation occurs, hence the relative stability of C_{60}^+ against ISRF. Pertinently, the absence of a detectable bottom-up benzene ring(s) generation scenario in the diffuse ISM is tentatively supported by C_{60}^+ being the sole carrier for a few DIBs (see §3), and a hitherto lack of convincing matches between DIBs and smaller or intermediate-sized PAH cations (e.g., Salama et al. 1999). For sizable PAHs, detectability prospects are counterbalanced by increasing isomer populations (e.g., Dias 1982), thus tentatively hinting why identifications have yet to emerge. Alternatively, Kwok (2022) and Kwok & Sadjadi (2023) highlight pitfalls endemic to the canonical PAH hypothesis, and champion MAONs (mixed aromatic/aliphatic organic nanoparticles).

The C≡N radical is of particular interest because Majaess et al. (2025c) identified its vibrational signature in a histogram of DIB energy differences, which remained prominent after noise analysis (500-4000 cm^{-1} range). DIBs may represent a vibrational progression, where energy differences between interrelated DIBs sharing a common carrier may reveal infrared vibrational transitions (e.g., Jenniskens & Desert 1993; Bondar 2020). Majaess et al. (2025c) proposed that a histogram tied to energy differences between highly correlated DIB pairs across the entire APO catalog may broadly reveal bonds endemic to the sources (e.g., aromatics, oop C−H bending, C−H stretch, C⁼C in-ring, overtones and combinations), thus circumventing challenging comparisons to individual molecules. For example, the Majaess et al. (2025c) analysis exposed the signatures of aromatics and C≡N (potentially nitriles given the former). Majaess et al. (2025c) conveyed the effort was a first macro exploratory step requiring independent validation and continuous fine-tuning. The analysis relied on the Pearson−r correlation coefficient[1], whereby $r = -1$ is a perfect inverse correlation, $r = 0$ indicates no correlation, and $r = +1$ is an ideal positive correlation, which characterizes the linear dependence between separate DIBs. The results conveyed in §2 indicate that the uncovered C≡N may be associated with larger PAHs, MAONs, and/or possibly endohedral or hetero fullerenes (e.g., Omont 2016).

In this study, experimental, computational, and observational findings (e.g., the expansive APO DIB catalog) were mobilized to assess the comparative presence of $C_6H_5CN^+$ in the diffuse ISM, thereby constraining molecular demographics in that specific environment by process of elimination. Experimental spectra are utilized that bypass matrices introducing sizable λ-shifts, which complicate DIB matching (e.g., neon matrix, tens of Ångströms, Bréchignac & Pino 1999), hence the advantage of the Daly et al. (2024) laboratory results exploited here. By comparison, DIBs can be on the order of Ångströms (e.g., Bondar 2012; Fan et al. 2019, the latter being the APO DIB catalog). Complementary synthetic spectra provide detailed characterizations of the transitions (e.g., D0-D3, Fig. 1), and the reader is referred to the following works for pertinent astrochemistry insights gleaned from quantum chemistry (Fortenberry 2021; Zapata Trujillo et al. 2023; Esposito et al. 2024). This initiative stemmed from a broader effort to delineate families of interrelated diffuse interstellar bands (DIBs) and scrutinize candidate molecular carriers (e.g., Seuret et al. 2025, see also Bondar 2012; Smith et al. 2021, 2022; Ebenbichler et al. 2024; Omont 2024). However, false positives are common (e.g., molecules increasing in tandem), and a mitigation strategy is to employ parts of a challenging multidimensional approach (r EW pairs, $|\Delta r|$ EW-E(B − V), potentially spectral morphology and FWHM, origin-band approach, optimal experimental spectra, etc., e.g., Galazutdinov et al. 2008).

2. Analysis

Our analysis aims to evaluate the detectability of $C_6H_5CN^+$ in the diffuse ISM, which may lend further support to a top-down hypothesis (excluding ion-dipole reactions) or a bottom-up pathway where aromatic molecules might assemble under such conditions.

Interrelated DIBs possibly stemming from a common carrier were identified on the basis of equivalent widths (EWs) exceeding Pearson $r \gtrsim 0.8$, relative to a DIB selected as the normalizing line ($\lambda_E \simeq 5602.0$ Å, Table 1 in Daly et al. 2024, not He tagged). This laboratory feature was chosen because of its proximity to DIB 5600.72 Å, and focused characterization by Daly et al. (2024). To mitigate false positives whereby highly correlated DIBs are tied to separate molecules whose abundances are commensurate, an absolute difference criterion was adopted between their EW correlations relative to optical reddening E(B-V) ($|\Delta r| \lesssim 0.3$). DIBs tied to the same molecular carrier should share a common correlation with reddening, and not necessarily a high correlation. The Fan et al. (2019) APO DIB catalog was analyzed, and only EWs with uncertainties were assessed, in tandem with a minimum sightline sampling criterion ($n \geq 8$). Unweighted correlations were evaluated. The sightline to VI Cyg 12 was excluded because it features excess reddening beyond the field and may host a circumstellar shell (e.g., Maryeva et al. 2016; Xing et al. 2024). For broader discussions regarding DIB EW and reddening correlations, see Smith et al. (2021) and Smith et al. (2022).

Experimental $C_6H_5CN^+$ spectra yield lines comparable in wavelength to DIBs at 5600.72 Å ($\lambda_E \simeq 5602.0$ Å) and 5594.58 Å ($\lambda_E \simeq 5595.3$ Å). These peaks could shift depending on the temperature and other considerations (Daly et al. 2024, their Fig. 5 and Table 1). The mean EWs for the DIBs are 3 and 6 mÅ, accordingly. EW ratios for 5594.58 and 5600.72 Å are offset (2.87 ± 0.37) from the near-unity that describes the experimental intensity ratios presented in Figs. 4 & 5 in Daly et al. (2024), and a high correlation ($r \simeq 0.9$) is juxtaposed upon a significantly offset ΔEW-E(B − V) correlation, thereby favoring separate carriers increasing in commensurate fashion. The conclusion would benefit from independent data. The comparison is indirect between experimental intensity and observed EWs, and offsets are expected. There is a general absence of matches elsewhere relative to observed EW and lab intensity ratios (Fig. 1). The

[1] defined as $r = \sum(x_i - \bar{x})(y_i - \bar{y}) / \sqrt{\sum(x_i - \bar{x})^2 \sum(y_i - \bar{y})^2}$

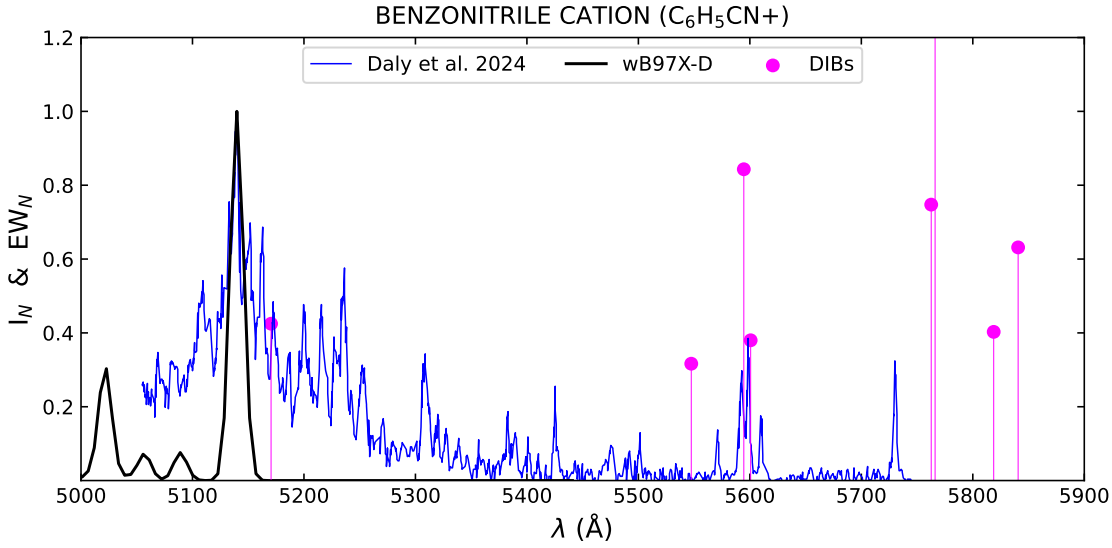

Figure 1. Mismatches exist between observed DIBs (the expansive APO catalog), and ωB97X-D/cc-pVTZ and experimental spectra. Experimental $C_6H_5CN^+ - He$ data (blue line, merely broadly illustrative) were inferred from a diagram in Daly et al. (2024). APO DIBs shown exhibit $r \gtrsim 0.8$ relative to 5600.72 Å (EW pairs, $n \geq 8$), and $|\Delta r| \lesssim 0.3$ between EW−E(B-V). Ultimately, solely two DIBs align with no less than ten experimental lines, which when paired with benzonitrile cation's IVR (Allain et al. 1996; Montillaud et al. 2013) and lack of recurrent fluorescence (§2.1), suggest in tandem with other evidence that the molecule is comparatively absent from the diffuse ISM.

$C_6H_5CN^+ - He$ data in Fig. 1 were inferred from a Daly et al. (2024) diagram using PlotDigitizer, and provide a broadly qualitative proxy relative to $C_6H_5CN^+$ (comparisons in Table 1 of Daly et al. 2024). An APO DIB exists slightly blueward of 5600.72 Å at 5599.76 Å (see also Table 3 in Daly et al. 2024), with half the EW, and it is unclear if they represent one line (e.g., DIBs 5779.59 and 5780.64 Å, see Smith et al. 2021). A DIB at 5609.82 Å is comparable to $\lambda_E \simeq 5613.1$ Å, yet the intensity to EW ratio differs from experimental spectra. Nevertheless, in tandem with a low vibrational well to store excess photon energy (e.g., Allain et al. 1996), Fig. 1 seemingly implies $C_6H_5CN^+$ is unlikely to exist in detectable quantities in the diffuse ISM. That assertion is not tied to specific environments around emission-based celestial targets (UIEs).

The generated spectrum for the D0-D3 transition is shown in Fig. 1. These simulated results were zero-pointed (λ) to the experimental D0-D3 and normalized to $\simeq$ 5140 Å. The experimental data do not sample the forbidden D0-D1 origin band, which is predicted near $\simeq$ 5803.9 Å (Xu et al. 2006). The DIB observations are not complicated by telluric contamination or blinding, as noted for the inconclusive C_{70}^+ case (Majaess et al. 2025a, see also the experimental data and interpretation of Campbell et al. 2016). Daly et al. (2024) articulated that the absence of DIBs near $\simeq$ 5140 Å may arise from observational constraints (i.e., large FWHM).

Density functional theory was used to generate theoretical spectra using the ωB97X-D long-range corrected density functional and the Dunning correlation-consistent cc-pVTZ basis set. The ground state D0 (X^2B_1) of $C_6H_5CN^+$ was optimized at this level of theory with a C2v symmetry point group, and frequency calculations were performed to ensure that it constituted a potential energy surface minimum. The relevant electronic energy level scheme is shown in Fig. 3 in Daly et al. (2024). Time-dependent DFT (TD-DFT) at the same level of theory with 10 excited states was also undertaken. From this analysis, and as Daly et al. (2024) mentioned, D0-D1 and D0-D2 are both electronically forbidden. An $f = 0.1$ oscillator strength characterizes the D0-D3 transition (ωB97X-D/cc-pVTZ). All calculations were performed using Gaussian 16 Rev. C.02 (Frisch et al. 2016). The TD-DFT spectrum computed here supports the presence of symmetry-allowed and forbidden electronic transitions reported in the experimental work.

In sum, Fig. 1 juxtaposes DIBs from the APO catalog with an experimental $C_6H_5CN^+ - He$ spectrum, and ωB97X-D/cc-pVTZ results. Possibly two DIBs align with no less than ten experimental lines. Lowering the liberal $|\Delta r|$ EW-E(B − V) criterion results in even less overlap.

2.1. Improbable Recurrent Fluorescence

McGuire et al. (2018) discovered that models were unable to explain the abundance of benzonitrile observed in TMC-1, a cold dense molecular cloud. The observed abundance was a factor of four larger than predictions, and hence pertinent formation pathways were missing. Subsequent work surmised that perhaps the shortfall could be addressed by benzonitrile cations in the diffuse ISM, and that fragmentation implied by the $C_6H_5CN^+$ IVR could be bypassed via recurrent fluorescence (see also the cyanonaphthalene research of Stockett et al. 2023). Daly et al. (2024) noted that hypothesis should be explored.

The lowest emissive electronic state should lie < 2.0 eV above the ground state for plausible recurrent fluorescence to occur (Haufler et al. 1991; Lacinbala et al. 2023), and PAH cations associated with naphthalene, cyanonaphthalene, anthracene, and perylene exhibit $\lesssim$ 1.9 eV gaps (Tokmachev et al. 2010; Martin et al. 2013; Saito et al. 2020; Daly et al. 2023). However, calculations here indicate that the lowest transition between two states for $C_6H_5CN^+$ (D0-D3) is 2.54 eV, which is analogous to the 2.58 eV reported in Fig. 3 of Daly et al. (2024). Therefore, the $C_6H_5CN^+$ transition is substantially higher than known recurrent fluorescence systems and is unlikely to be efficiently thermally

populated. Moreover, this insight is paired with benzonitrile not adhering to a homogeneous trend in distribution maps of TMC-1 (Cernicharo et al. 2023), which disfavors the cation as the key donor. Benzonitrile in TMC-1 follows overdensities that likewise feature cyanopolyynes, and Cernicharo et al. (2023) conclude that aromatics in TMC-1 are formed from smaller molecules in the densest regions of the cloud (i.e., not benzonitrile cations). Furthermore, the smaller benzonitrile features far fewer vibrational modes than the aforementioned larger PAHs (inadequate energy diffusion via IVR) and are struck by unceasing high-energy dissociating photons prior to or approximately concurrent with bottom-up encounters in the diffuse ISM. Dissociative recombination is also a pertinent factor.

It has been suggested that the lack of DIB matches to experimental $C_6H_5CN^+$ may arise because of the molecule's low oscillator strength and observational limitations, and the abundance of benzonitrile cations may be due to recurrent fluorescence. Here, we propose a separate position, whereby recurrent fluorescence is improbable in this instance, and based on the broader holistic evidentiary framework, the benzonitrile cation is relatively absent in the diffuse ISM.

3. Conclusion

The benzonitrile cation is comparatively absent in the diffuse ISM owing to a marginal vibrational diffusion mechanism for excess photon energy (Allain et al. 1996; Montillaud et al. 2013), improbable recurrent fluorescence (§2.1), unceasing photon strikes, and general mismatches between the experiment and observed DIBs (Fig. 1). These findings, in concert with the current lack of DIBs linked to comparably sized molecules, reaffirm the gaps inherent to bottom-up synthesis. Critically, low oscillator strength may inhibit the detection of molecules in the pathway sequence when relying solely on DIB matching; however, this limitation can be partially overcome by instituting the aforementioned holistic scaffolding and recognizing that presently, only C_{60}^+ is attributed to a few DIBs (see below).

Future work should examine whether the advocated falsification strategy is meritorious and can be extended to intermediate-size aromatic nitriles. Essentially, the broader objective is to have detectability constraints spanning molecular size, environmental conditions, and ionization state, as well as recurrent fluorescence and IVR efficiencies. Concurrently, future efforts to characterize DIBs include ongoing research on fullerenes, especially from the perspective of endohedral and hetero fullerenes (e.g., Omont 2016, and references therein), and with respect to bolstering the C_{60}^+ case. Majaess et al. (2025a) unveiled that the existing controversy regarding the two most prominent DIBs linked to C_{60}^+ (9577 and 9632 Å) likely stemmed from each team's data occupying a narrow dynamic range, and establishing a broad EW baseline confirmed the aforementioned lines exhibit a high correlation (Fig. 1 in Majaess et al. 2025a). However, a match to C_{60}^+ cannot merely rest on two lines, and consequently, Majaess et al. (2025b) examined one of three weaker lines likewise debated in the literature, and produced amongst the first explicit Pearson correlation linked to a relevant sample size (i.e., 9365 − 9577 Å are highly correlated, Fig. 2 in Majaess et al. 2025b). Yet, the Majaess et al. (2025b) intercomparison of various published spectra revealed inhomogeneities leading them to agree with Galazutdinov et al. (2021) that evidence for the remaining two weaker lines was unconvincing (9348 − 9428 Å), and Majaess et al. (2025b) explicitly noted that additional research is needed on those two lines to mitigate false positives from overlapping PAHs (or potentially MAONs). Concerning C_{70}^+, a trio of Campbell et al. (2016) experimental wavelengths match DIBs within an Ångström (Majaess et al. 2025a), however, numerous challenges underscored by Majaess et al. (2025a) render that candidate carrier uncertain (see also the interpretation of Campbell et al. 2016). First, a suite of prominent lines could be obscured by telluric contamination (Campbell et al. 2016) and hinder the necessary full comparison, thus requiring (in)validation by space-based measurements (e.g., Cordiner et al. 2019). Second, the low EWs complicate correlation analyses and indirect comparisons of observed EW ratios relative to experimental intensity attenuation ratios (mismatched, see Table 4 and Fig. 2 in Majaess et al. 2025a), especially since FWHM is challenging to determine in low-EW circumstances and certain lines may be incomplete or bifurcated (see §2.2 in Majaess et al. 2025a). Work on all these diverse areas (& more) is desirable.

This study relied on initiatives such as the APO DIB catalog, CDS, NASA ADS, arXiv, Gaussian 16, ChemCompute+GAMESS (Perri & Weber 2014), and experimental spectra from the ISLA (Campbell) group.

REFERENCES

Allain, T., Leach, S., & Sedlmayr, E. 1996, A&A, 305, 602
Bondar, A. 2012, MNRAS, 423, 725, doi: 10.1111/j.1365-2966.2012.20910.x
—. 2020, MNRAS, 496, 2231, doi: 10.1093/mnras/staa1610
Bréchignac, P., & Pino, T. 1999, A&A, 343, L49
Campbell, E. K., Holz, M., Gerlich, D., & Maier, J. P. 2015, Natur, 523, 322, doi: 10.1038/nature14566
Campbell, E. K., Holz, M., Maier, J. P., et al. 2016, ApJ, 822, 17, doi: 10.3847/0004-637X/822/1/17
Cernicharo, J., Tercero, B., Marcelino, N., Agúndez, M., & de Vicente, P. 2023, A&A, 674, L4, doi: 10.1051/0004-6361/202346722
Cordiner, M. A., Linnartz, H., Cox, N. L. J., et al. 2019, ApJ, 875, L28, doi: 10.3847/2041-8213/ab14e5
Crawford, M. K., Tielens, A. G. G. M., & Allamandola, L. J. 1985, ApJ, 293, L45, doi: 10.1086/184488
Daly, F. C., Douglas-Walker, T. E., Palotás, J., et al. 2024, JChPh, 161, 074305, doi: 10.1063/5.0223270
Daly, F. C., Palotás, J., Jacovella, U., & Campbell, E. K. 2023, A&A, 677, A128, doi: 10.1051/0004-6361/202347199
Di Giacomo, F. 2015, JChEd, 92, 476, doi: 10.1021/ed5001312
Dias, J. R. 1982, Journal of Chemical Information and Computer Sciences, 22, 15, doi: 10.1021/ci00033a004
Ebenbichler, A., Smoker, J. V., Lallement, R., et al. 2024, A&A, 686, A50, doi: 10.1051/0004-6361/202348871
Esposito, V. J., Fortenberry, R. C., Boersma, C., Maragkoudakis, A., & Allamandola, L. J. 2024, MNRAS, 531, L87, doi: 10.1093/mnrasl/slae037
Fan, H., Hobbs, L. M., Dahlstrom, J. A., et al. 2019, ApJ, 878, 151, doi: 10.3847/1538-4357/ab1b74
Fortenberry, R. 2021, in 43rd COSPAR Scientific Assembly. Held 28 January - 4 February, Vol. 43, 1986
Frisch, M. J., Trucks, G. W., Schlegel, H. B., et al. 2016, Gaussian 16 Revision C.02
Galazutdinov, G. A., LoCurto, G., & Krełowski, J. 2008, ApJ, 682, 1076, doi: 10.1086/589758

Galazutdinov, G. A., Valyavin, G., Ikhsanov, N. R., & Krełowski, J. 2021, AJ, 161, 127, doi: 10.3847/1538-3881/abd4e5
Harriott, T., Rahi, Q., Seuret, H., et al. 2025, in AAS Meeting Abstracts, Vol. 245, AAS Meeting Abstracts #245, 202.12
Haufler, R. E., Chai, Y., Chibante, L. P. F., et al. 1991, JChPh, 95, 2197, doi: 10.1063/1.460968
Heger, M. L. 1922, LicOB, 10, 146
Jenniskens, P., & Desert, F. X. 1993, A&A, 274, 465
Kwok, S. 2022, Ap&SS, 367, 16, doi: 10.1007/s10509-022-04045-6
Kwok, S., & Sadjadi, S. 2023, in American Astronomical Society Meeting Abstracts, Vol. 241, American Astronomical Society Meeting Abstracts #241, 144.07
Lacinbala, O., Calvo, F., Dartois, E., et al. 2023, A&A, 671, A89, doi: 10.1051/0004-6361/202245421
Majaess, D., Harriott, T. A., Seuret, H., et al. 2025a, MNRAS, 538, 2392, doi: 10.1093/mnras/staf425
—. 2025b, RNAAS, 9, 248, doi: 10.3847/2515-5172/ae0572
Majaess, D., Seuret, H., Harriott, T. A., et al. 2025c, MNRAS, 539, 3489, doi: 10.1093/mnras/staf722
Marcus, R. A. 1952, JChPh, 20, 359, doi: 10.1063/1.1700424
Martin, S., Bernard, J., Brédy, R., et al. 2013, PHRvL, 110, 063003, doi: 10.1103/PhysRevLett.110.063003
Maryeva, O. V., Chentsov, E. L., Goranskij, V. P., et al. 2016, MNRAS, 458, 491, doi: 10.1093/mnras/stw385
McGuire, B. A., Burkhardt, A. M., Kalenskii, S., et al. 2018, Sci, 359, 202, doi: 10.1126/science.aao4890
Montillaud, J., Joblin, C., & Toublanc, D. 2013, A&A, 552, A15, doi: 10.1051/0004-6361/201220757
Omont, A. 2016, A&A, 590, A52, doi: 10.1051/0004-6361/201527685
—. 2024, A&A, 690, A275, doi: 10.1051/0004-6361/202450841
Perri, M. J., & Weber, S. H. 2014, JChEd, 91, 2206, doi: 10.1021/ed5004228
Saito, M., Kubota, H., Yamasa, K., et al. 2020, PhRvA, 102, 012820, doi: 10.1103/PhysRevA.102.012820
Salama, F., Galazutdinov, G. A., Krełowski, J., Allamandola, L. J., & Musaev, F. A. 1999, ApJ, 526, 265, doi: 10.1086/307978
Seuret, H., Sullivan, A. D., Morera-Boado, C., et al. 2025, PCCP, 27, 12666, doi: 10.1039/D4CP04023F
Smith, E. R., Smith, F. M., Harriott, T. A., et al. 2022, RNAAS, 6, 82, doi: 10.3847/2515-5172/ac680f
Smith, F. M., Harriott, T. A., Majaess, D., Massa, L., & Matta, C. F. 2021, MNRAS, 507, 5236, doi: 10.1093/mnras/stab2444
Stockett, M. H., Bull, J. N., Cederquist, H., et al. 2023, NatCo, 14, 395, doi: 10.1038/s41467-023-36092-0
Tokmachev, A. M., Boggio-Pasqua, M., Mendive-Tapia, D., Bearpark, M. J., & Robb, M. A. 2010, JChPh, 132, 044306, doi: 10.1063/1.3278545
Weisman, J. L., Lee, T. J., Salama, F., & Head-Gordon, M. 2003, ApJ, 587, 256, doi: 10.1086/368103
Xing, H., Sullivan, A., Seuret, H., et al. 2024, RNAAS, 8, 90, doi: 10.3847/2515-5172/ad380d
Xu, H., Johnson, P. M., & Sears, T. J. 2006, JChPh, 125, 164331, doi: 10.1063/1.2355675
Zapata Trujillo, J. C., Pettyjohn, M. M., & McKemmish, L. K. 2023, MNRAS, 524, 361, doi: 10.1093/mnras/stad1717